PROCEEDINGS OF SCIENCE

A macroscopic model of radar detection for the Radar Echo Telescope

Enrique Huesca Santiago[a,*] **and Krijn de Vries**[a] **on behalf of the Radar Echo Telescope Collaboration**
(a complete list of authors can be found at the end of the proceedings)
[a] *Vrije Universiteit Brussel - Interuniversity Institute for High Energy physics (VUB -IIHE), Pleinlaan 2, Brussels, Belgium*
E-mail: ehuescasantiago@gmail.com, krijndevries@gmail.com

We introduce a new macroscopic model to simulate in-ice radar detection of high-energy particle cascades in dense media. High energy cosmic ray showers impacting a high altitude ice sheet, or cosmic neutrinos interacting in the ice produce a high-energy particle cascade, which leaves a short-lived plasma trail composed of ionized ice electrons. Unlike direct radio detection methods, the RET experiment aims to use radar technique to detect the particle cascade via the reflection of radio waves off this plasma.

The new semi-analytical description presented in this work is based on well-known parametrizations of the cascade's charge distribution and uses first-principles derivations for the estimated radar cross section of a full cascade scatter. The model includes all the known relevant physics that will affect the radar signal, such as the free charge collisional damping, electron lifetime, and relativistic effects due to the cascade propagation.

9th International Workshop on Acoustic and Radio EeV Neutrino Detection Activities (ARENA 2022)
7 - 10 June 2022
Santiago de Compostela, Galicia, Spain

*Speaker

PoS(ARENA2022)017

1. Introduction

The IceCube Neutrino Observatory has, at this time, only detected a handful of neutrino events with an energy above 1 PeV (= 10^{15} eV) [1]. The goal of the Radar Echo Telescope (RET) experiment is to detect cosmic neutrino-induced particle cascades at even higher energies, above the PeV region [2]. The radar echo technique is based on the reflection of radio waves off the ionization trail left by a cascade front passing through the ice. Each high-energy particle in the shower front is expected to ionise about $O(10^5)$ low-energy electrons per cm from the medium, and each electron is expected to live $O(1-10$ ns$)$. The ionisation, low-energy, electron trail from the cascade front can be described as a low density plasma. This plasma is what ultimately scatters off the radio waves, producing the radar echo.

Earlier efforts of astroparticle radar detection comprise the detection of extensive air showers (EAS) induced from cosmic-rays; and it has been deemed unfeasible [3] [4] due to the low electron density left in the wake of the EAS. The extended EAS trail makes the local electron density insufficient to overcome the collisional damping with the air molecules. The first in-ice radar scatter model [5] estimated that the increased medium density of the ice allows for a more efficient scatter of radio waves, making radar detection possible. This radar echo has been observed in the laboratory, within a test beam experiment [6]. The current phase of the RET experiment is geared towards RET-CR: the first in-nature detection of the radar echo from a high-energy particle cascade. RET-CR aims to detect cosmic-ray EAS cores penetrating a high altitude ice surface. RET-CR will serve both as definitive proof of concept of the radar echo technique and as a pathfinder for a future neutrino experiment - RET-N. For more information on the RET experiment, see references [7] [8] [9].

The standard use of the radar echo method is to measure the power scattered from a macroscopic metallic object, characterised by its radar cross section (RCS). The RCS of a perfect electric conductor of typical size l, $l >> \lambda_{radio}$, can (generally) be reduced to its projected surface area as seen from the transmitter. On the other hand, we know the classical (low energy) RCS for a single, free electron; the *Thomson scattering cross section* $\sigma_{Th} \sim 10^{-29}$ m^2. A 10 PeV particle cascade traversing the ice will leave a footprint of $O(10^{14})$ ionised electrons. These plasma-like electrons, surrounded by ice molecules, do not make for a perfectly electric conductor. Additionally, their sheer number makes the single-particle treatment of each ionised electron in the cascade numerically intractable. Furthermore, the cascade front is moving relativistically, so the length and time scales of the plasma are correlated in a geometry-dependent fashion. This rules out Rayleigh scattering and other classical treatments of the scatter process and makes the analytical treatment of the cascade's σ_{RCS} impracticable.

In this work we introduce a complete *semi-analytical*, macroscopical model of the radar scatter in ice. This model relies on a parametrisation of the in-ice cascades, and is a promising way to gain a deeper understanding of the physical processes that influence the final signal at the receiver. This model is expected to coexist along, and agree with, RadioScatter, the current Monte-Carlo (MC) standard [10] [11], and as a non-MC calculation of radar echo, it will give us a fast way to simulate events in the RET telescope for optimisation and reconstruction purposes.

2. The neutrino-induced particle cascade

Particle cascade EAS models have been developed for decades [13], both empirical and first-principles parametrisations, up to and including recent efforts to model the EAS impacting and continuing though the ice [12]. The cascades used in this work are are described by the long-standing NKG parametrisation, where the longitudinal profile is given by Greisen [13]:

$$N(X) = \frac{0.31}{\sqrt{\ln(E/E_{crit})}} e^{X/X_0(1-1.5\ln(s))}, \tag{1}$$

and the lateral distribution of particles is taken from Nishimura and Kamata [14],

$$w(r,s) = \frac{\Gamma(4.5-s)}{\Gamma(s)\Gamma(4.5-2s)} \left(\frac{r}{r_0}\right)^{s-1} \left(\frac{r}{r_0}+1\right)^{s-1}. \tag{2}$$

The parameters in these models are usually defined for air. Here, we adapt them for the ice medium instead. Our working values are: The critical energy $E_{crit} = 78.6$ MeV; the moliere radius $r_0 = 7$ cm; and the interaction length $X_0(ice) = 36.08 \mathrm{g/cm^2} \simeq X_0(air)$ [5] .

The local density of the trail electron plasma can be found by:

$$n_{e,plasma} = \frac{E_{deposited} = 2 \text{ MeV/cm}}{E_{ionisation} = 20 \text{ eV}} * n_{HE} \left[\frac{g}{\mathrm{cm^3}}\right] \simeq 10^5 * \frac{1}{V} \int_L N(l, E_p) dL \int_R w(r,s) dr. \tag{3}$$

and it is shown in Fig 1 below:

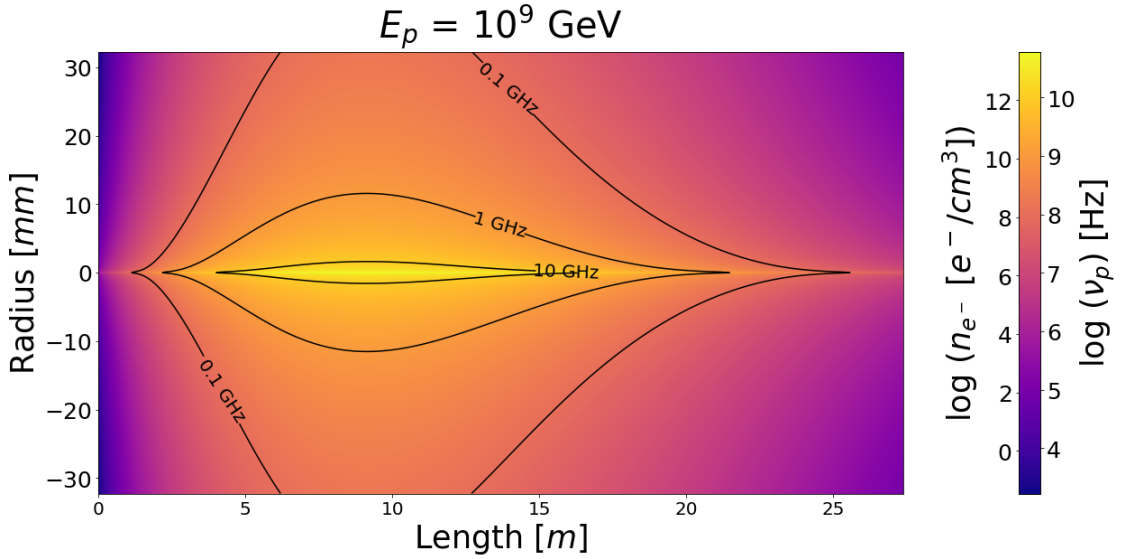

Figure 1: The electron plasma density profile of a 1 EeV NKG particle cascade in ice. Note the difference in units in both axis. The local electron density can also be represented via the *plasma frequency* $\nu_p = 8980\sqrt{n_e}$ [Hz]. The three black lines represent the traditional "overdense" ($\nu_p > \nu_{TX}$) regions at different probing frequencies ν_{TX}, under the assumption of no collisional damping.

3. Radar Scattering of particle cascades

Radar scattering is characterised by the radar range equation:

$$P_{RX} = P_{TX}\frac{G_{TX}G_{RX}\lambda^2}{(4\pi)^3(R_{TX}R_{RX})^2} * \sigma_{RCS} * [f_{att}(R)] * [f_{pol}]. \tag{4}$$

The received power P_{RX}, is a function of the transmitted power P_{TX}; the gain of the transmitter and receiver antennas, G_{TX}, G_{RX}; the distances of both antennas to the scattering element, R_{TX}, R_{RX}; and the wavelength λ of the radio wave. The radar cross section σ_{RCS}, which has units of area, represents the "equivalent scattering area". While the polarisation efficiency f_{pol}, and the medium attenuation efficiency f_{att} are vital for a complete description, they will be left out in the following discussion.

Nearby electrons will scatter coherently if, by definition, the differences in their retarded fields are negligible. This happens for all electrons under a typical distance l which must be smaller than a wavelength λ [15]. This means that an arbitrarily small volume $\leq l \sim 1\ cm^3$ can be understood as a single scattering centre including all the particles within it.

Each scattering centre contributes with their own scattering strength, E_{sc}, and their phase ($\phi = kR - \omega t|_{RX} + \psi$); where the phase, evaluated at the receiver's clock ($t|_{RX}$) accounts for retardation effects ($t|_{RX} = t|_{sc} + R_{RX}/c_{ice}$) and ψ denotes the freedom for each centre to gain its individual phase shift (if required). Using the linearity of the electric fields, the returned electric field is the sum of the fields of the scattering centres.

$$P_{RX} \propto |\vec{E}_{RX}(R,t)|^2 = \left|\sum_{i=1}^{N} E_{sc,i}(R_i,t) * e^{i(kR_i - \omega t|_{RX} + \psi_i)}\right|^2 \tag{5}$$

To summarise, in our macroscopic approach, the solution for the cascade scatter is found by numerically combining the individual, non-relativistic scattering centres, for which an analytical solution (as shown below) exists. All the associated relativistic effects of the radar scatter stem from the interference of these phases. For example, Cherenkov-like features are expected in our signal.

To that purpose, we need an "electric field radar range equation", the equation of the amplitude of the electric field at the receiver that is consistent with Eq. 4, the original radar range equation. By considering the antennas that emit and record the signals, with Z the free space impedance, and A_{RX} the effective area of the receiver, we have

$$P_{RX} = \frac{E^2}{2Z}A_{RX} \rightarrow E^2 = \frac{2ZP}{A_{RX}} = 2ZP\left(\frac{4\pi}{\lambda^2 G_{RX}}\right), \tag{6}$$

which makes the electric field at the receiver:

$$E_{RX} = \frac{1}{4\pi R_{TX}R_{RX}}\sqrt{2Z_{ice}P_{TX}G_{TX}}\sqrt{\sigma_{RCS}}. \tag{7}$$

3.1 The electric field from a single particle

We are left to find the electric field scattered by N scattering centres. First, we consider the electric field scattered by a single electron, for which an analytical solution is known. Inside the area illuminated by the transmitter, the local electric field seen by the electron is E_e:

$$|E_e| = \sqrt{2ZI_e} = \sqrt{2Z_{ice}I_0\mathcal{T}} = \sqrt{2Z_{ice}\mathcal{T}\left(\frac{P_{TX}G_{TX}}{4\pi R_{TX}^2}\right)}. \tag{8}$$

The magnitude of the electric field can be obtained from the power transmitted (P_{TX}) via the local irradiance, I_e. Within the cascade, the local irradiance is the irradiance "outside"[1] the cascade (I_0) times the cascade transparency $\mathcal{T}$ (see next section).

The local electric field exerts a force $\vec{F} = qE_e\cos(kR_{TX} - \omega t)\hat{E}$ on the ionised electrons, which try to move in the dense ice media. During its ionised lifetime, $O(1-10)$ ns, the electron is expected to undergo $O(10^5)$ elastic collisions with the ice molecules. This introduces the collisional damping term with an associated frequency ω_{colls}. Overall, the movement of the electron can be described as damped-driven oscillator. The amplitude of those oscillations is:

$$|x_e| = \frac{qE_e}{m}\left(\frac{1}{\omega^2 - i\omega\omega_{coll}}\right) = \frac{qE_e}{m}W = A_0W \tag{9}$$

A_0 would be the amplitude for the non-collisional case, while W captures the damping ratio.

The electric field from a single electron at a receiver RX is given by [15], Eq. 3.15:

$$\vec{E}_{e,RX} = \frac{q}{(4\pi\epsilon_0)c^2R_{RX}}[\hat{n}\times(\hat{n}\times\hat{\hat{x}}_e)] = \frac{q\omega^2}{(4\pi\epsilon_0)c^2R_{RX}}x_e(t_{ret})\sin(\theta_{RX})\hat{\theta}, \tag{10}$$

with θ_{RX} is the angle between the direction of oscillation, $\hat{x}_e$, and the direction of the receiver $\vec{e}_{RX} = \hat{k}_e$; and $\hat{\theta} = \hat{\theta} \perp \hat{k}_e$ is the direction of the field arriving to the antenna.

Putting together Eqs. 9 and 10, we now obtain:

$$\begin{aligned} |E_e|_{RX} &= \frac{q\omega^2}{(4\pi\epsilon_0)c^2R_{RX}}|x_e(t_{ret})\sin(\theta)|[f_{pol}] = \frac{r_e}{R_{RX}}(|E_e|\omega^2W)|\sin(\theta)|[f_{pol}] \\ &= |E_e|(\omega^2W)\frac{1}{R_{RX}}\sqrt{\sigma_{Th}\frac{1}{4\pi}G_{Hz}}[f_{pol}] \end{aligned} \tag{11}$$

We have chosen to rewrite the equation in terms of the Thomson cross section $\sigma_{Th} = \frac{8\pi}{3}r_e^2$ and the *Herztian dipole gain factor* $G_{Hz} = \frac{3}{2}sin^2(\theta)$. This way, all of our constants add up to the *classical electron radius* ($r_e \sim 2.8\cdot10^{-15}$ m). The exact shape of the *polarisation factor* f_{pol}, as well as any *medium attenuation factor*, $f_{att} = f_{att}(R,\omega)$ are model-dependant and being omitted for our current discussion.

[1] A cascasde plasma has no clearly defined outer boundaries, "outside" here refers to the radio wave unaffected by the bulk of the cascade electrons.

Combining Eq. 8 with Eq. 11, we arrive to:

$$|E_e|_{RX} = \frac{\sqrt{2ZP_{TX}G_{TX}}}{4\pi R_{TX}R_{RX}}\sqrt{(\omega^2 W)^2\sigma_{Th}G_{Hz}\mathcal{T}}[f_{pol}f_{att}]. \tag{12}$$

If we compare Eq. 12 to Eq. 7, we find the expression for the radar cross section of the damped electron:

$$\sigma_{RCS,e} = (\omega^2 W)^2\sigma_{Th}G_{Hz}\mathcal{T}. \tag{13}$$

Last, if we are assuming a collection of coherently scattering electrons, the electric field scales with the number of electrons. All those electrons are assumed to be excited at a time t_0 and then exist in the ionised state with an average lifetime of τ_e. The final amplitude of the electric field of a scattering centre consisting of N_e coherently scattering particles now becomes:

$$E_{sc} = E_e \cdot N_e \cdot e^{-\frac{t}{\tau}} \cdot \Theta(t - t_0). \tag{14}$$

We can define the associated σ_{RCS} of the scattering centre as:

$$\sigma_{RCS,sc} = \sigma_{Th}N_e^2(\omega^2 W)^2\mathcal{T} \cdot G_{Hz} \cdot e^{-\frac{2t}{\tau}}\Theta(t - t_0) \tag{15}$$

From Eqs. 14 and 5 we can now obtain the return electric field at the receiver for the full shower in $O(10^6)$ calculations.

4. The role of transparency in the energy balance of the scatter.

The macroscopic understanding of the scatter comes from medium polarisation. A standard argument is that the bulk of ionised electrons change the index of refraction of the medium, n. In our plasma, $\mu = \mu_0$ and $\epsilon = \epsilon_0(1 + \chi_e)$, the dispersion relation becomes ([16], Eq. 7.51):

$$k = \frac{\omega}{c}\left[1 + \omega_p^2 W\right]^{1/2} \simeq \frac{\omega}{c}\left[1 + \frac{1}{2}\omega_p^2 W\right] = Re(k) + iIm(k). \tag{16}$$

The propagating radio wave ($\vec{k}$) gains an imaginary term, the *plasma attenuation* β:

$$\beta = 2Im(k) = 2\frac{\omega}{c}Im(n) \simeq \frac{\omega}{c}\omega_p^2 Im(W) = \frac{\omega_c}{c}(\omega\omega_p W)^2. \tag{17}$$

It is trivial to verify that $\mathrm{Im}(W) = \omega\omega_c W^2$. The attenuation determines the (macroscopic) power decrease of the radio waves when considered along a (macroscopic) path. This is the *radio transparency*, $\mathcal{T}$:

$$P(z) = P_0 e^{\int_0^z -\beta(l)dl} = P_0\mathcal{T} \tag{18}$$

The attenuation of radio wave going through a plasma volume V of thickness l and area A is:

$$\mathcal{P}_{att} = \frac{\Delta P}{V} = \frac{1}{V} * P_0(1 - \mathcal{T}) = \frac{I * A}{A * l} * (1 - e^{-\beta l}) \sim \frac{I}{l}\beta l = I\beta \tag{19}$$

To first order, the power density that is attenuated is linear with the incident irradiance and the plasma attenuation. Also worth noting, the attenuation is defined by the three typical frequencies

of the system: The transmitted angular frequency ω; the plasma angular frequency ω_p, and the collision angular frequency ω_c, as $W = W(\omega, \omega_p, \omega_c)$. Therefore, we can derive the attenuation of our plasma, as shown in Fig. 2 from its electron density (Fig. 1) for a given set of $(\omega_c, \omega = \omega_{TX})$.

Complementary to a macroscopic perspective, we can derive the attenuation from single-electron scattering model. The scattering is understood as the absorption and re-emission of the incoming radio wave, so here the attenuation is a measure of the power loss via the damped-driven oscillator. The energy that the radio wave loses to scattering per electron is given by:

$$\langle P(t) \rangle = \frac{1}{2m} (qE_0 \omega W)^2 \omega_c. \tag{20}$$

The power lost in a system of N_e electrons is $P = \langle P(t) \rangle N_e$, and the power density is $\mathcal{P} = \langle P(t) \rangle n_e$, with n_e the electron number density. Therefore, the transferred power density is:

$$\mathcal{P}_{loss} = \frac{1}{2} \left(\frac{n_e q^2}{m} \right) (E_0 \omega W)^2 \omega_c = \frac{1}{2} \epsilon_0 (\omega_p E_0 \omega W)^2 \omega_c = I * \left(\frac{\omega_c}{c} (\omega \omega_p W)^2 \right) = I\beta, \tag{21}$$

making the model of the damped-driven oscillator consistent under power conservation (the power absorbed by the bulk volume matches that of the scattering by the electrons within it). It follows that neither collisional damping nor the transparency can be neglected when modelling the scatter.

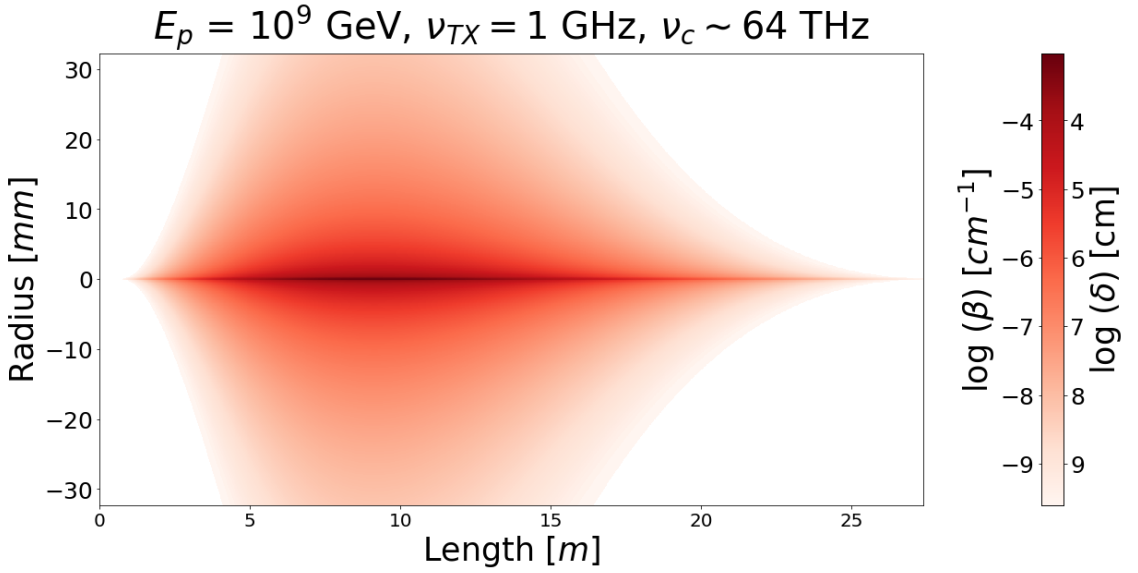

Figure 2: The attenuation profile associated with the density distribution of Fig 1. The attenuation can be better understood by its inverse, the *skin depth* δ, the distance that it would take to the incoming wave to lose $1/e$ of its power. At the core, which is only a few cm in diameter, δ is O(100) m, which means that the cascade is highly transparent and the incoming wave will only lose a small fraction of its power to the radar echo.

5. Conclusions

The radar echo technique is a novel idea to detect in-ice trails from high-energy particle cascades. The in-ice cascades can be described with the same parametrisations as their EAS counterparts, which gives us the local electron density of the cascade trail. We introduce here a new semi-analytical method to fully describe the radar scatter off this trail, where the standard radar range equation needs to be applied in a numerical fashion over small collections of coherently scattering electrons. An outline of the expected radar cross section of these elements is derived, under the scattering model of the damped-driven oscillator. The damped-driven oscillator scattering model is consistent under power conservation with the textbook definitions of the macroscopic radio attenuation.

References

[1] R. Abbasi *et al* (IceCube Collaboration), Phys. Rev. D, **104**, 2 (2021), 022002
[2] Radar Echo Telescope. https://www.radarechotelescope.org, access date: 1st of June, 2022.
[3] J. Stasielak *et al*, Astropart. Phys. **73**, (2016), 14 - 27
[4] TARA collaboration, Astropart. Phys. **87**, (2017), 1 - 17
[5] K. D. de Vries, K. Hanson, and T. Meures, Astropart. Phys. **60**, (2015), 25 - 31
[6] S. Prohira, K. de Vries *et al*, Phys. Rev. Lett, **124**, 9 (2020), 091101
[7] S. Prohira *et al* (RET collaboration), Phys. Rev. D, **104**, 10 (2021), 102006
[8] R. Stanley *et al*. (RET collaboration), PoS **ARENA2022**, 009 (2022)
[9] V. Lukic *et al*. (RET collaboration), PoS **ARENA2022**, 010 (2022)
[10] S. Prohira, RadioScatter repository
[11] S. Prohira and D. Besson, Nucl. Instrum. Methods. Phys. Res. A (2018) 161 - 170
[12] S. De Kockere, K. D. de Vries, N. van Eijndhoven, U. A. Latif, Phys. Rev. D **106**, 043023 (2022) 043023.
[13] Wilson J. G. and Greisen K. Progress in cosmic ray physics. Vol. 3. Ed: North-Holland (1956).
[14] Koichi Kamata and Jun Nishimura, Prog. Th. Phys. Supplement. **6** (1958) 93 – 155
[15] G.B. Rybicki and A. P. Lightman . Radiative process in astrophysics. Ed: Wiley, 2nd edition (2004).
[16] J. D. Jackson. Classical Electrodynamics. Ed: Wiley, 3rd edition (1999).

PoS(ARENA2022)017

Full Authors List: Radar Echo Telescope Collaboration

S. Prohira[1], K.D. de Vries[2], P. Allison[3], J. Beatty[3], D. Besson[1], A. Connolly[3], A. Cummings[4], P. Dasgupta[5], C. Deaconu[6], S. De Kockere[2], D. Frikken[3], C. Hast[7], E. Huesca Santiago[2], C.-Y. Kuo[8], U.A. Latif[2], V. Lukic[2], T. Meures[9], K. Mulrey[10], J. Nam[8], K. Nivedita[10], A. Nozdrina[3], E. Oberla[6], J.P. Ralston[1], C. Sbrocco[3], M.F.H. Seikh[1], R.S. Stanley[2], J. Torres[3], S. Toscano[5], D. Van den Broeck[2], N. van Eijndhoven[2], and S. Wissel[4]

[1]University of Kansas, Lawrence, KS, USA [2]Vrije Universiteit Brussel, Brussel, Belgium [3]Department of Physics, Center for Cosmology and AstroParticle Physics (CCAPP), The Ohio State University, Columbus, OH, USA [4]Departments of Physics and Astronomy & Astrophysics,Institute for Gravitation and the Cosmos, Pennsylvania State University, University Park, PA, USA [5]Université Libre de Bruxelles, Brussels, Belgium [6]Enrico Fermi Institute, Kavli Institute for Cosmological Physics,Department of Physics, University of Chicago, Chicago, IL, USA [7]SLAC National Accelerator Laboratory, Menlo Park, CA, USA [8]National Taiwan University, Taipei, Taiwan [9]University of Wisconsin-Madison, Madison, WI, USA [10]Radboud University, Nijmegen, Netherlands

PoS(ARENA2022)017